Abstract

The microexplosion evolution phenomenon of single droplets of water in pure diesel emulsion under Leidenfrost effect has been studied. The tested emulsions were stabilized with a blend of commercial surfactants with three different water contents of 9%, 12% and 15%. A high speed camera synchronized with backlight technique was used to capture the evolution of microexplosion and puffing. Three different droplet diameters of approximately 2.6mm, 2mm and 0.2mm were analysed. It was found that the tendency of microexplosion and puffing frequency was influenced by the droplet diameter. Coalescence was the dominating factor in inducing microexplosion in bigger droplets. It was observed that the child droplets ejected from the parent droplet undergoes further puffing processes.The size of the secondary droplets after microexplosion were also found to be slightly influenced by the parent droplet size.The waiting time for microexplosion and puffing were compared for different droplets size.

Keywords

Microexplosion, Leidenfrost Effect, Coalescence, Surfactant, Sauter Mean Diameter (SMD)

Introduction

In spite of their preferable advantages, diesel engines are one of the foremost pollution contributors to the environment (Basha and Anand, 2011, Brijesh et al., 2015). One way to combat these drawbacks of compression ignition (CI) engines can be overcome by fuel based solutions, which can be readily adapted to the existing engines without any modifications. Emulsified fuels are considered as one of the conceivable alternative fuels for reducing the engine exhaust emissions (Abu-Zaid, 2004, Armas et al., 2005, Park et al., 2000, Yahaya Khan et al., 2014). The most noticeable effects of such fuels are the secondary atomization occurring during the combustion process. The volatility difference between the base fuel and the dispersed water droplets (i.e) results in superheating of the water which is achieved before

the base fuel and rapid vapour expansion which leads to a violent microexplosion of the emulsified droplets (Watanabe et al., 2010) . The presence of water aids to reduce the combustion temperature, therefore reducing NOx. The microexplosion phenomena results in the formation of smaller droplets with very high surface-to-volume ratio which results in better mixing with air leading to more complete combustion and lower particulate matter (PM) emissions.

The microexplosion phenomenon is often quoted for countering the engine exhaust emissions (i.e.) reducing PM and NO_x simultaneously. Therefore, understanding the microexplosion phenomena can help to increase the efficiency of alternative fuels, in particular with water in diesel emulsions. Usage of suspended droplets on thermocouple or quartz fiber has been studied previously to record the temperature history of the heated emulsion droplets,(i.e) emulsion of pyrolysis oil in diesel oil (Calabria et al., 2007) , n-dodecane and n-tetradecane in water emulsion (Tsue et al., 1996), kerosene and water emulsion (Watanabe et al., 2009), commercial diesel and water emulsion (Califano et al., 2014), and diesel- bio diesel-ethanol blends (Avulapati et al., 2016). One of the main demerits in these type of techniques is that the presence of thermocouple or the fiber wire results in the heterogeneous bubble nucleation on the surface of the wire (Watanabe et al., 2010). A 50µm diameter R-type thermocouple was used in their study. On the other hand Mura (Mura et al., 2014) concluded that the presence of 76.2µm diameter K-type thermocouple did not dominate the microexplosion process. However, the size, geometry and of heat transfer to the thermocouple from the droplet and its effect on the microexplosion evolution is still unclear.

Also, prior studies confirmed that the microexplosion does not always occur (Califano et al., 2014, Khan et al., 2014, Yahaya Khan et al., 2016). The droplet diameters considered for the purpose of visualization of the microexplosion evolution were different among the studies.

Emulsion fuels with the parent droplet size, studied previously by the other researchers for the development of microexplosion phenomenon are highlighted in the Table 1. This experimental work investigates the evolution of microexplosion phenomenon of water in pure diesel emulsion droplets. Breakup characterisation studies of child droplets are scarce and are limited to base fuels other than pure diesel (Avulapati et al., 2016). Such characteristics are also studied here by analyzing the primary and secondary droplet sizes in order to fill in this gap in the knowledge base. The droplets sizes studied in this experiment are within the comparable range of other researchers, so as to compare the present results with their works.

[Insert Table-1]

Reference	Emulsion fuels used	Parent droplet diameter (mm)
(Ocampo-Barrera et al., 2001)	Heavy fuel oil/water	0.83
(Tanaka et al., 2006)	n-dodecane + n-tetradecane + n-hexadecane + water	2
(Watanabe et al., 2009)	kerosene/water	0.7-1.3
(Morozumi and Saito, 2010)	n-hexadecane/water	1.5-1.8
(Suzuki et al., 2011)	kerosene/water	0.85-0.99
(Tarlet et al., 2014)	sunflower oil/water	0.15-0.45
(Califano et al., 2014)	commercial diesel/water	0.7-1.1
(Mura et al., 2014)	sunflower oil/water	1

Materials and methods

Emulsion preparation and stability

The Water in Diesel Emulsions (WiDE) used in this study was blended at 1500rpm for 15 minutes using overhead stirrer. Mixtures of commercial surfactants Span-80 with an HLB value of 4.3 and an HLB of 11 for TWEEN 85 were used as emulsifier. Surfactants are necessary to lower the interfacial tension between the diesel and water to form a stable emulsion. The base fuel used was pure diesel without any additives. The emulsions were

stabilized with 15% of surfactant concentration to the water content. The preparation matrix for the WiDE is shown in Table 2. All the prepared emulsions were found to be stable for almost 30 days. This was due to the dosage of surfactant blend being sufficient to the overall surface of the dispersed compound to be completely covered by the surfactant molecules (Abdul Karim et al.).

A Hydrophilic-Lipophilic Balance (HLB) value of 9 was used for stabilizing all the emulsions. It was obtained by mixing the two surfactants by the following equation

$$\% A = 100 * (\times - HLB_B)/(HLB_A - HLB_B) \quad (1)$$

Where

HLB_A = HLB value of surfactant A

HLB_B = HLB value of surfactant B

x = Required HLB value

$\% A$ = Quantity of surfactant A required

$\% B$ = Quantity of surfactant B required (i.e) (% B=100- % A)

[Insert Table-2]

Experimental Setup

Schematic diagram of the experimental setup for the evolution of microexplosion visualization is shown in Figure 1. The basic principle of the setup is same as that of Mura (Mura et al., 2012). A PHANTOM MIRO M310 high speed camera was used for image capturing. The image acquisition rate was set at 8000 fps for larger droplets and 10000 fps with a resolution of 640X480 for droplets with the smallest diameter. A polished flat aluminum plate with a small concave dint was used to place the droplet and the base plate

temperature was maintained at 500 +/- 2°C using a ceramic heater to obtain the Leidenfrost effect. The temperature was maintained throughout the experiment by a digital temperature controller. The water droplets distribution images were captured by using a digital microscope with a magnification of 1000X and the Sauter mean diameter of dispersed water droplets were calculated by post processing the images obtained. The light source used for backlight illumination purpose was of single LED type and was synchronized with the exposure time of the high speed camera. Also, a light source with 12 high power LEDs was used for direct image recording to observe the phase changes and internal features of the droplet during the evolution of microexplosion. The recording speed was set at 2000 fps with a resolution of 510X510 pixels. The images were post processed using the phantom camera control software for measurements and calculating the waiting time of microexplosion. Approximately 2.6 mm and 2 mm sized droplets diameters of water in pure diesel emulsion (WiDE) were generated using a syringe of 0.8mm and 0.4mm orifice diameter needles. Due to the limitations in the generation of smaller droplets. A single bigger emulsion droplet of diameter 2.6mm was made to fall on the heated aluminium plate from a height, which results in immediate shattering of bigger droplet in to numerous smaller droplets of diameter approximately 0.2mm. It should be noted that if the created smaller droplets are not formed of emulsions it will not develop microexplosion. On the other hand if the droplets are formed only with pure diesel it will not under go microexplosion phenomenon, instead it will only evaporate (Khan et al., 2014). Each emulsion sample was tested three times under same testing conditions to ascertain the behaviour. The high speed camera was set to start recording the events as soon as the droplet touched the hot plate. This was achieved by the pre-trigger option available with camera control software. This facilitated the identification of the exact starting time during post processing of the captured images.

[Insert Figure -1]

Results and discussion

The water droplet distribution in the emulsions was captured using a digital microscope with a magnification of 1000X as shown in Figure 2. The water droplet diameter measurements were made using the Motic Image plus 2.0 software.

[Insert Figure -2]

The sizes of the measured droplets were expressed in terms of Sauter Mean Diameter (SMD) (D_{32}) as follow:

$$D_{32} = \sum_i (n_i \times D_i^3) / \sum_i (n_i \times D_i^2) \quad (2)$$

Where D_i is the diameter of the droplet and n_i is the total number of droplets having the same diameter. The size distribution of water droplets of the samples are depicted in Figure 3. It is clear from Figure 3 that WiDE-1 had a wide range of distributed water droplet diameters even with sizes of 7.6 to 8.4 μm. Whereas, WiDE-2 had 0.8 to 1.2 μm and WiDE-3 had 0.8 to 1.4μm diameter droplets which were more densely populated.

For the same surfactant dosage, the SMD of WiDE-1 was around 6 μm, 3.34 μm for WiDE-2 and 3.65 μm WiDE-3 as shown in Figure 4. In the case of WiDE-1, a uneven size distribution of a wide range droplet diameters were present. Whereas, the difference between the droplet diameters for WiDE-2 and WiDE-3 were very small. According to Mura, in his studies on microexplosion of water in sunflower oil, the uneven distribution of bigger droplets leads to faster coalescence and eventually microexplodes. (Mura et al., 2012).

[Insert Figure -3]

[Insert Figure -4]

[Insert Table -3]

Physical properties of the prepared emulsions are tabulated in the Table 3. The density of the emulsions was found to be almost the same for all the WiDE samples and the viscosity was increasing with increasing water content. The surface tension of WiDE-1 was lower compared to the other two samples.

Microexplosion evolution of WiDE with bigger parent droplet

The evolution of WiDE Ø2.6 mm (approx.) size droplets is shown in Figure 5. Since no significant changes in the emulsion phase were observed in the early part of the experiment after the placing of the droplet on the surface, the image sequence shown is from 2 seconds onwards and was captured using the direct image recording.

[Insert Figure -5]

[Insert Figure -6]

The rate of coalescence to form larger dispersed water droplets was found to be more dominant (as highlighted in Figure 6) in the emulsion WiDE-1 with 9% water, hence more readily exploded when compared to the other two WiDE samples. The size of the coalescenced water droplets was in the range of 650 μm to 1000 μm for WiDE-1, 69 μm to 37 μm for WiDE-2 and it was between 37 μm to 105 μm in case of WiDE-3. The phase change for all the WiDE with Ø2.6mm is shown in Figure 6 for selected times. It is clear from these images that the coalescence is more dominant in case of WiDE-1 than the other two emulsions. Also, the coalescence leading to phase change occurred earlier than the other WiDE emulsions**.** As shown in Figure 3, WiDE-1 contains a wide range of different sized dispersed water droplets compared to the other two WiDE samples. This non uniform distribution of water droplets led to a higher coalescence rate and hence resulted in microexplosion. Whereas, the other two WiDE samples had narrow sized distributed water

droplets, with a minimum difference in the values of the SMD, did not undergo intensive coalescence resulting in only phase change with no microexplosion. Similar behaviour was observed for all the three trials.

[Insert Figure -7]

[Insert Figure -8]

The sequence of evolution of the Ø2.0 mm is shown in Figure 7. The images shown are from 0 second and with a time interval of 0.5 seconds. Similar behaviour occurred in the case of droplets with Ø2.0 mm (approx.) in which WiDE-1 developed microexplosion whereas the other two emulsions did not. The secondary droplets after microexplosion from WiDE-1 are shown in Figure 8. Further observation of the secondary droplets from a Ø2.6 mm parent droplet were in the average size of Ø0.22 mm with a standard deviation of 0.181 and the secondary droplets from the Ø2.0 mm parent droplet were around Ø0.19 mm with a standard deviation of 0.112. From these observations implies that the size of the secondary droplets is slightly influenced by the size of the parent droplet itself. However, more tests has to be performed to confirm this precisely.

[Insert Figure -9]

[Insert Figure -10]

Figures 9 and 10 depict the changes in the diameter of the parent droplet at half second time interval. For both cases there were no significant changes in the droplet diameter up to 1.5 s, due to the fact that the droplet might not had enough heating energy. As the time increases the droplet diameter started increasing due to vapour expansion inside the droplet. As the pressure

built up in the droplet and reached a particular point water leaves the droplets in a very fine mist (Ochoterena et al., 2010). Puffing is the ejection of the inner content of the emulsified droplet without the complete shattering of the parent droplet. At the end of every puffing (resulting in ejection of larger child droplets) the diameter of the parent droplet dropped and underwent further vapour expansion and its diameter increased as shown in the graph. The time taken for initial puffing and the puffing frequency of Ø2.0 mm and Ø2.6 mm WiDE droplets are shown in Figure 11.

The time taken for initial puffing was found to increase with increasing water content in the case of Ø2.6 mm droplet diameter whereas no such trend was observed in the case of Ø2.0 mm diameter droplets. However, it is clear from the Figure 11 that the time taken for the initial puffing was considerably less in the case of smaller droplet of WiDE.

[Insert Figure -11]

As far as the puffing frequency is concerned, it was comparatively higher for the Ø2.6 mm droplet than the Ø 2.0 mm. Notably, WiDE-3 with 15% water content exhibited maximum puffing frequency irrespective of the droplet diameters. It was found that the parent droplet size played an important role in the puffing frequency with the larger parent droplets producing high puffing frequencies.

As highlighted in the Figure 12, the child droplets ejected from the parent droplet during puffing was observed to undergo further puffing. The ejected child droplet was about Ø0.568 mm. The child droplet was ejected at 1.590s from the parent droplet and the puffing time for the child droplet was at 1.5921s.

[Insert Figure -12]

Microexplosion and puffing behaviour of smaller WiDE droplets

The microexplosion evolutions of the smaller droplets of Ø0.2 mm to Ø0.3 mm are discussed in this section. These droplets were generated by dropping a larger droplet from a height onto the hot plate which resulted in the production of smaller droplets.

[Insert Figure -13]

Since it was not possible to control the size or the movement of the droplets generated this way, only selected droplets which underwent microexplosion were considered for analysis excluding bouncing droplets. These images were captured at 10000 fps. The microexplosion behaviour of smaller droplets of WiDE-1, 2 and 3 are shown in Figure 13.

[Insert Table - 4]

[Insert Figure -14]

The waiting times of the parent droplets and the size of the secondary droplets after microexplosion are shown in Table 4. The secondary droplets created after microexplosion of parent droplets were between 1/3 and 1/10 of the size of the parent droplets. Figure 14 shows the instantaneous images of a puffing sequence of WiDE-2, which was observed with the smaller parent droplet of Ø0.2 mm and resulted in child droplets of Ø0.135 mm and Ø0.138 mm. The duration of puffing was 0.002 s. As shown in Figure 14, the diameter of the parent droplet increased due to vapour expansion and resulted in the puffing of child droplets. The ejected child droplets were observed to undergo further puffing processes as shown.

Conclusions

Water in pure diesel emulsion (WiDE) with different parent droplet sizes were visualized for the microexplosion evolution and the outcomes of the observation are summarised as follows;

- Coalescence and the size of the coalescenced water droplet was the dominant factor in inducing the microexplosion phenomenon in the case of large droplets.

- Puffing frequency of the WiDE droplets was found to be a function of the parent droplet size.
- The chid droplets ejected during puffing of parent droplets underwent further puffing processes.
- Unlike the large diameter droplets, the small sized (Ø0.2 mm) WiDE droplets developed microexplosion irrespective of their water content.
- The size of the child droplets after microexplosion was almost less than 1/10 of the size of the parent droplet for large droplets (Ø2.6 and Ø2.0 mm) and between 1/3 and 1/10 of the size of the smaller parent droplet. The present testing conditions implies that the size of the secondary droplets is slightly influenced by the size of the parent droplet itself. However, further tests has to be performed to confirm this precisely.

Acknowledgements

The authors wish to thank the Universiti Teknologi PETRONAS for the financial and facility support for the study. The authors express their gratitude to Firmansyah and Ezrann Zharif for their technical assistance in conducting the experiments.

References

ABDUL KARIM, Z. A., KHAN, M. Y., A. AZIZ, A. R. & TAN, I. M. 2014. Characterization of Water in Diesel Emulsion. *MATEC Web of Conferences,* 13**,** 02006.

ABU-ZAID, M. 2004. Performance of single cylinder, direct injection diesel engine using water fuel emulsions. *Energy Conversion and Management,* 45**,** 697-705.

ARMAS, O., BALLESTEROS, R., MARTOS, F. & AGUDELO, J. 2005. Characterization of light duty diesel engine pollutant emissions using water-emulsified fuel. *Fuel,* 84**,** 1011-1018.

AVULAPATI, M. M., GANIPPA, L. C., XIA, J. & MEGARITIS, A. 2016. Puffing and micro-explosion of diesel–biodiesel–ethanol blends. *Fuel,* 166**,** 59-66.

BASHA, J. S. & ANAND, R. 2011. An experimental study in a CI engine using nanoadditive blended water–diesel emulsion fuel. *International Journal of Green Energy,* 8**,** 332-348.

BRIJESH, P., CHOWDHURY, A. & SREEDHARA, S. 2015. Advanced combustion methods for simultaneous reduction of emissions and fuel consumption of compression ignition engines. *Clean Technologies and Environmental Policy,* 17**,** 615-625.

CALABRIA, R., CHIARIELLO, F. & MASSOLI, P. 2007. Combustion fundamentals of pyrolysis oil based fuels. *Experimental Thermal and Fluid Science,* 31**,** 413-420.

CALIFANO, V., CALABRIA, R. & MASSOLI, P. 2014. Experimental evaluation of the effect of emulsion stability on micro-explosion phenomena for water-in-oil emulsions. *Fuel,* 117**,** 87-94.

KHAN, M. Y., ABDUL KARIM, Z. A., AZIZ, A. R. A. & TAN, I. M. 2014. Experimental Investigation of Microexplosion Occurrence in Water in Diesel Emulsion Droplets during the Leidenfrost Effect. *Energy & Fuels,* 28**,** 7079-7084.

MOROZUMI, Y. & SAITO, Y. 2010. Effect of physical properties on microexplosion occurrence in water-in-oil emulsion droplets. *Energy & Fuels,* 24**,** 1854-1859.

MURA, E., CALABRIA, R., CALIFANO, V., MASSOLI, P. & BELLETTRE, J. 2014. Emulsion droplet micro-explosion: Analysis of two experimental approaches. *Experimental Thermal and Fluid Science,* 56**,** 69-74.

MURA, E., MASSOLI, P., JOSSET, C., LOUBAR, K. & BELLETTRE, J. 2012. Study of the micro-explosion temperature of water in oil emulsion droplets during the Leidenfrost effect. *Experimental Thermal and Fluid Science,* 43**,** 63-70.

OCAMPO-BARRERA, R., VILLASENOR, R. & DIEGO-MARIN, A. 2001. An experimental study of the effect of water content on combustion of heavy fuel oil/water emulsion droplets. *Combustion and flame,* 126**,** 1845-1855.

OCHOTERENA, R., LIF, A., NYDÉN, M., ANDERSSON, S. & DENBRATT, I. 2010. Optical studies of spray development and combustion of water-in-diesel emulsion and microemulsion fuels. *Fuel,* 89**,** 122-132.

PARK, J., HUH, K. & PARK, K. 2000. Experimental study on the combustion characteristics of emulsified diesel in a rapid compression and expansion machine. *Proceedings of the Institution of Mechanical Engineers, Part D: Journal of Automobile Engineering,* 214**,** 579-586.

SUZUKI, Y., HARADA, T., WATANABE, H., SHOJI, M., MATSUSHITA, Y., AOKI, H. & MIURA, T. 2011. Visualization of aggregation process of dispersed water droplets and the effect of aggregation on secondary atomization of emulsified fuel droplets. *Proceedings of the Combustion Institute,* 33**,** 2063-2070.

TANAKA, H., KADOTA, T., SEGAWA, D., NAKAYA, S. & YAMASAKI, H. 2006. Effect of ambient pressure on micro-explosion of an emulsion droplet evaporating on a hot surface. *JSME International Journal Series B,* 49**,** 1345-1350.

TARLET, D., MURA, E., JOSSET, C., BELLETTRE, J., ALLOUIS, C. & MASSOLI, P. 2014. Distribution of thermal energy of child-droplets issued from an optimal micro-explosion. *International Journal of Heat and Mass Transfer,* 77**,** 1043-1054.

TSUE, M., KADOTA, T., SEGAWA, D. & YAMASAKI, H. Statistical analysis of onset of microexplosion for an emulsion droplet. Symposium (International) on Combustion, 1996. Elsevier, 1629-1635.

WATANABE, H., HARADA, T., MATSUSHITA, Y., AOKI, H. & MIURA, T. 2009. The characteristics of puffing of the carbonated emulsified fuel. *International Journal of Heat and Mass Transfer,* 52**,** 3676-3684.

WATANABE, H., SUZUKI, Y., HARADA, T., MATSUSHITA, Y., AOKI, H. & MIURA, T. 2010. An experimental investigation of the breakup characteristics of secondary atomization of emulsified fuel droplet. *Energy,* 35**,** 806-813.

YAHAYA KHAN, M., ABDUL KARIM, Z., AZIZ, A. R. A. & TAN, I. M. Experimental Study on Influence of Surfactant Dosage on Micro Explosion Occurrence in Water in Diesel Emulsion. Applied Mechanics and Materials, 2016. Trans Tech Publ, 287-291.

YAHAYA KHAN, M., ABDUL KARIM, Z., HAGOS, F. Y., AZIZ, A. R. A. & TAN, I. M. 2014. Current Trends in Water-in-Diesel Emulsion as a Fuel. *The Scientific World Journal,* 2014.

Table Caption

Table 1. Droplet sizes and emulsion fuels on previous studies

Table 2. The preparation matrix for the WiDE

Table 3. Physical properties of WiDE

Table 4. Waiting time of smaller droplets of WiDE

Table 1

Reference	Emulsion fuels used	Parent droplet diameter (mm)
(Ocampo-Barrera et al., 2001)	Heavy fuel oil/water	0.83
(Tanaka et al., 2006)	n-dodecane + n-tetradecane + n-hexadecane + water	2
(Watanabe et al., 2009)	kerosene/water	0.7-1.3
(Morozumi and Saito, 2010)	n-hexadecane/water	1.5-1.8
(Suzuki et al., 2011)	kerosene/water	0.85-0.99
(Tarlet et al., 2014)	sunflower oil/water	0.15-0.45
(Califano et al., 2014)	commercial diesel/water	0.7-1.1
(Mura et al., 2014)	sunflower oil/water	1

Table 2

Volume of surfactant	Sample ID	Amount of H_2O (ml)	Volume (ml)	
			Diesel	Surfactant
15% from H_2O	WiDE-1	9	89.65	1.35
	WIDE-2	12	86.20	1.8
	WIDE-3	15	82.75	2.25

Table 3

Sample ID	Density @ 20°C (g/m^3)	Viscosity @ 40°C (m pas)	Surface tension @ 20°C (mN/m)
Pure diesel	0.84376	2.7396	-----
WiDE-1	0.86109	3.4223	27.47
WiDE-2	0.86052	3.6863	32.27
WiDE-3	0.87140	4.6791	31.11

Table 4

Sample ID	Droplet diameter (mm)	Microexplosion time (s)	Average diameter of secondary droplets after microexplosion (mm)
WiDE-1	0.17	0.196	0.053
WiDE-2	0.23	0.152	0.031
WiDE-3	0.30	0.233	0.030

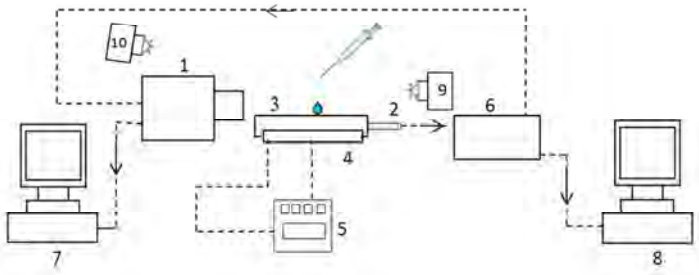

1. High Speed Camera 2. Thermocouple for hot plate 3. Hot plate 4.Ceramic heater 5. Temperature controller for hot plate 6. N.I.Controller 7&8. PC for Data Acquisition and Image processing 9. Light source for backlight illumination 10. Light source for front light illumination

Figure 1. Microexplosion visualization schematic diagram

338x190mm (96 x 96 DPI)

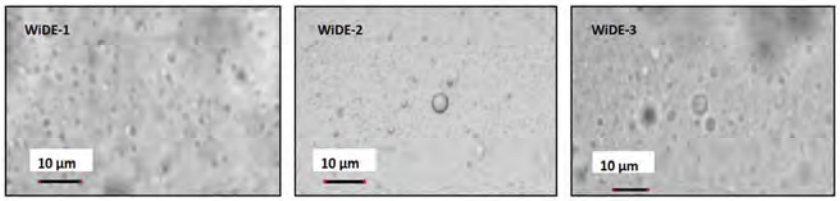

Figure 2. Images of WiDE, from left to right, with 9%, 12% and 15% water content

338x190mm (96 x 96 DPI)

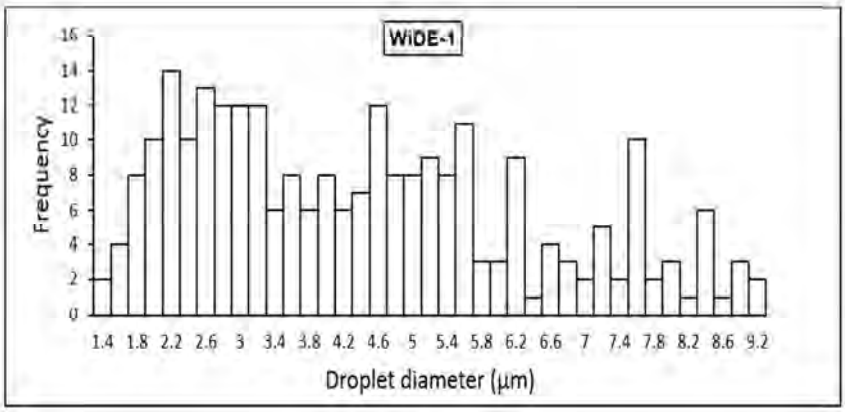

Figure 3. The size distribution of water droplets of WiDE samples

338x190mm (96 x 96 DPI)

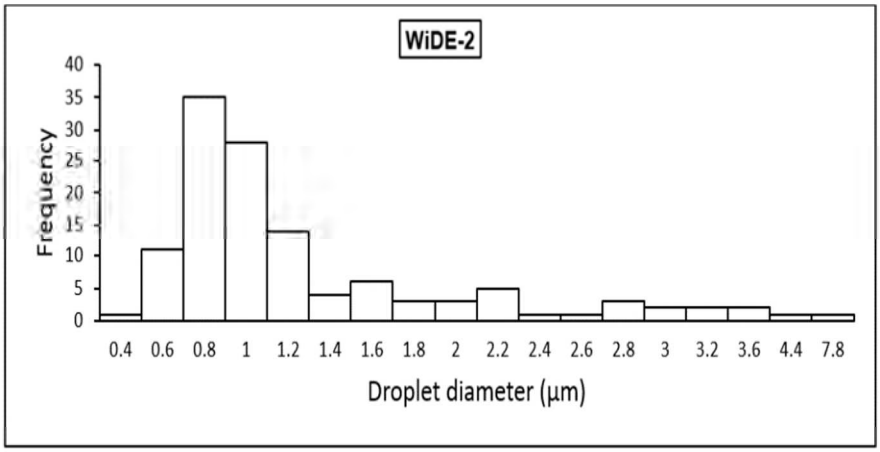

Figure 3. The size distribution of water droplets of WiDE samples

338x190mm (96 x 96 DPI)

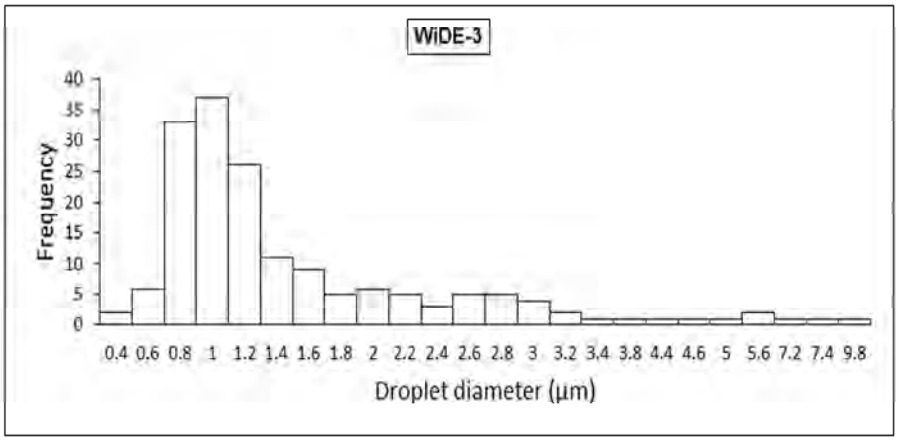

Figure 3. The size distribution of water droplets of WiDE samples

338x190mm (96 x 96 DPI)

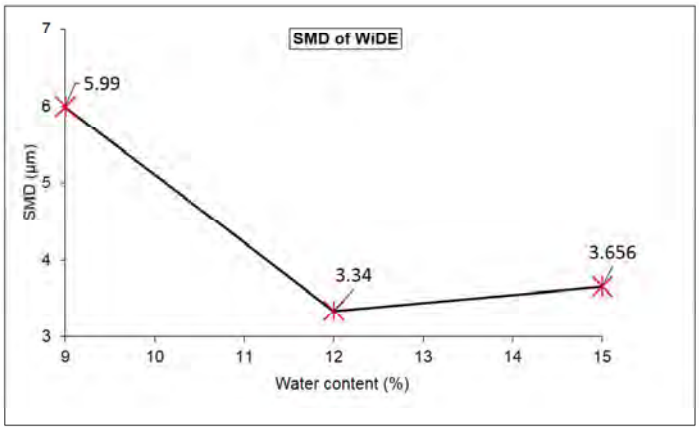

Figure 4. Sauter mean diameter (SMD) of WiDE vs water content

338x190mm (96 x 96 DPI)

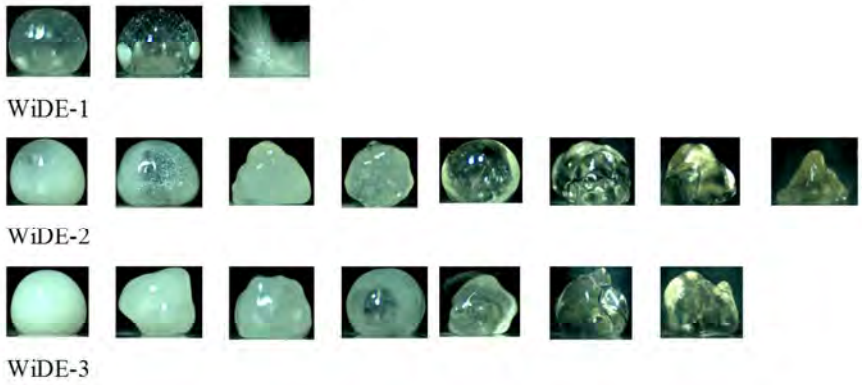

Figure 5. Evolution of ϕ2.6mm droplets WiDE-1, 2 and 3 at every 0.5s time interval

338x190mm (96 x 96 DPI)

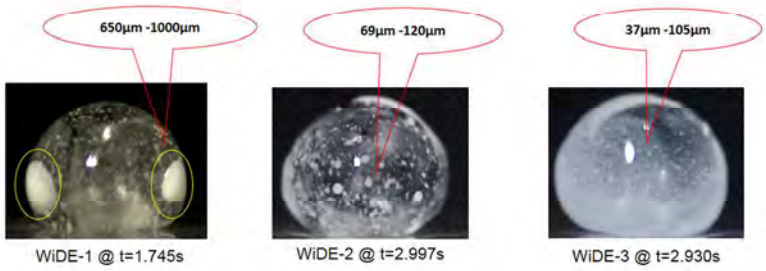

Figure 6. Images showing the phase change of emulsions with 9%, 12%, and 15% water content with time interval

338x190mm (96 x 96 DPI)

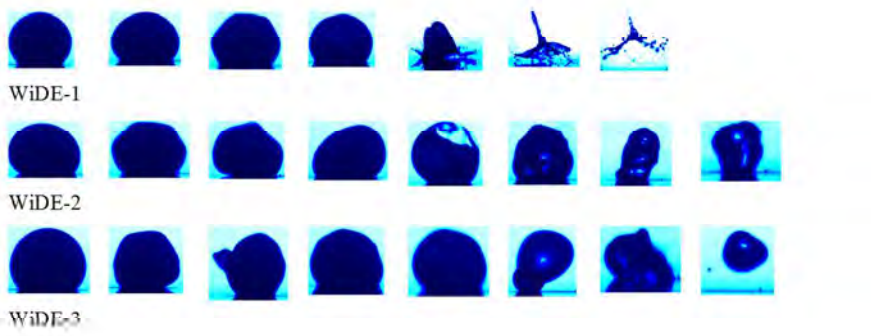

Figure 7. Evolution of ϕ2.0mm droplets WiDE-1, 2 and 3 at every 0.5s time interval

338x190mm (96 x 96 DPI)

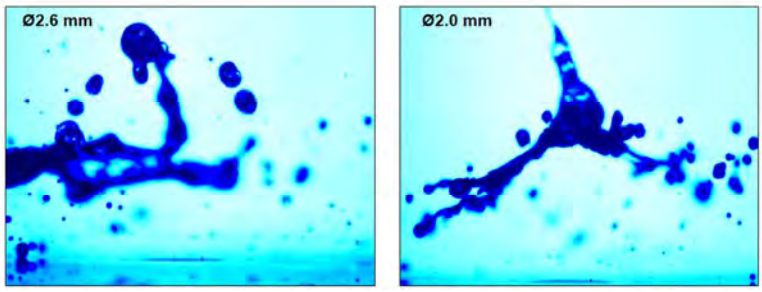

Figure 8. Secondary droplets after microexplosion of ϕ2.6mm and ϕ2.0mm WiDE-1 parent droplets

338x190mm (96 x 96 DPI)

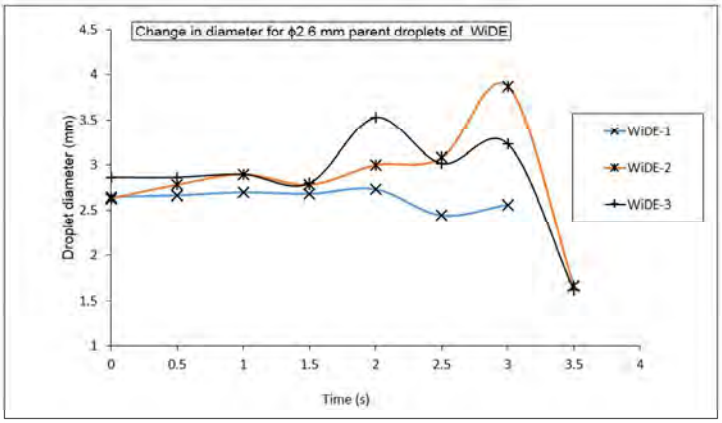

Figure 9. Change in diameter of ϕ2.6 mm WiDE droplets at every 0.5s interval

338x190mm (96 x 96 DPI)

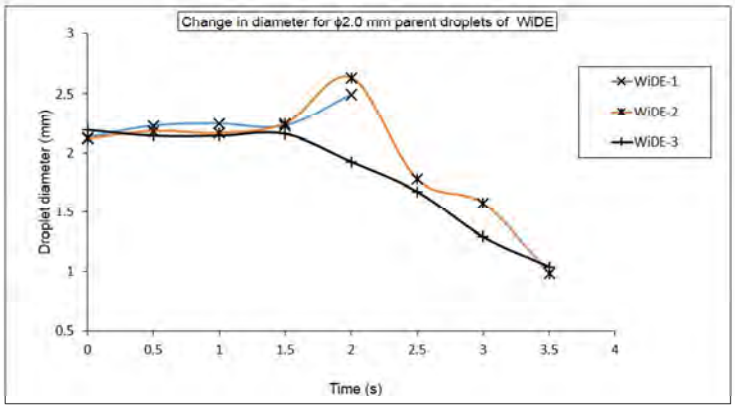

Figure 10. Change in diameter of ϕ2.0 mm WiDE droplets at every 0.5s interval

338x190mm (96 x 96 DPI)

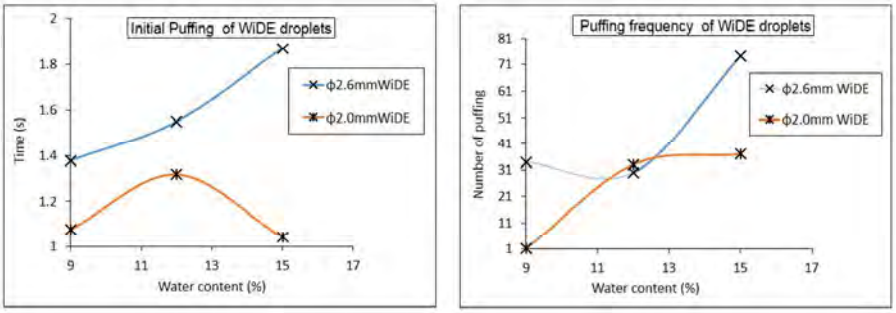

Figure 11. Time taken for initial puffing and the puffing frequency of ϕ2.6 mm and ϕ2.6 mm WiDE droplets

338x190mm (96 x 96 DPI)

Figure 12. Puffing of a child droplet of ϕ0.5681 mm ejected from of parent droplet of ϕ2.6 mm

338x190mm (96 x 96 DPI)

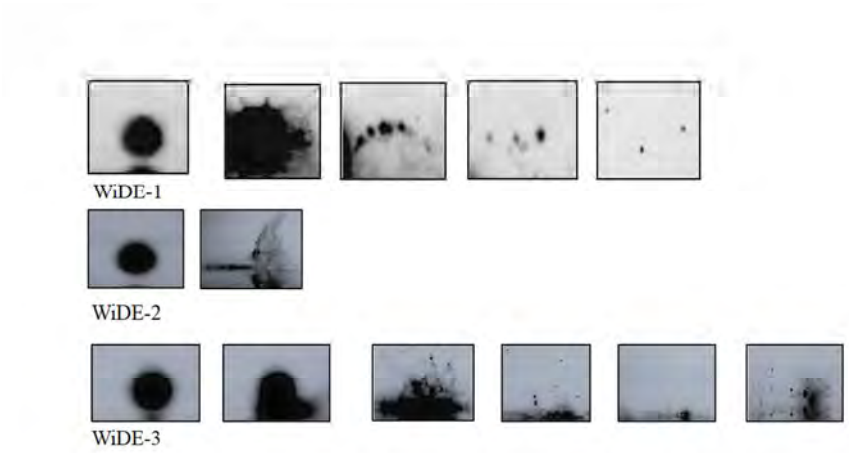

Figure 13. Microexplosion of smaller parent WiDE droplets and secondary droplets

338x190mm (96 x 96 DPI)

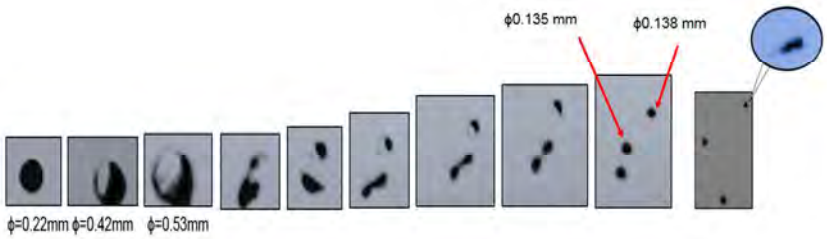

Figure 14. Puffing sequence of a parent droplet of diameter ϕ0.224mm, resulting in ejection of child droplets

338x190mm (96 x 96 DPI)